CHANGES IN THE SURFACE LAYER OF ROLLED BEARING STEEL

Oskar Zemčík*, Josef Chladil, Josef Sedlák

Institute of Manufacturing Technology, Technická 2896/2, Brno 616 69, Czech Republic

* corresponding author: zemcik.o@fme.vutbr.cz

Abstract. This paper describes changes observed in bearing steel due to roller burnishing. Hydrostatic roller burnishing was selected as the most suitable method for performing roller burnishing on hardened bearing steel. The hydrostatic roller burnishing operation was applied as an additional operation after standard finishing operations. All tests were performed on samples of 100Cr6 material (EN 10132-4), and changes in the surface layer of the workpiece were then evaluated. Several simulations using finite element methods were used to obtain the best possible default parameters for the tests. The residual stress and the plastic deformation during roller burnishing were major parameters that were tested.

Keywords: bearing steel; roller burnishing; finite element method; residual austenite; residual stress.

1. Race of a rolling-element bearings

Roller bearings form an integral part of a large number of machines and devices. They are widely used in the automotive industry, in transport machinery, in machine tools, in aerospace engineering, etc. Their mechanical properties and their reliability have a significant impact on the operation of the entire system. Various types of roller bearings are made, ranging from the most common ball bearings through tapered, cylindrical, and barrel bearings to special types for specific purposes. The critical factor is the dynamically loaded surface layer of the bearing ring. This is what ultimately leads to fatigue failure (see Fig. 1).

In the case of bearing rings made of bearing steel 14109 (DIN 1.3505 100Cr6) and 14209 (DIN 1.3520 100CrMn6), the layer is thermally treated, and is then ground and superfinished. To increase the life and the reliability of a roller bearing, the dynamically-loaded bearing surface may be submitted to roller burnishing, which improves the properties of the surface layer of the ring without actually changing the dimensions of a ring that has already been machine processed [11].

2. Hydrostatic roller burnishing

The roller burnishing method does not eliminate the total residual stress induced for example by previous grinding, but it causes compressive stresses by plastification of the surface layer [1, 3, 4, 9]. The compressive stresses on the surface of the burnished area then prevent the development of cracks and eliminate the effects of micronotches.

It is suitable to use a hydrostatic roller burnishing head with a ball-shaped element roughly 3 mm in diameter as a roller burnishing tool in for hardened bearing steel. Hydrostatic roller burnishing heads made by HEGENSCHEIDT or by ECOROLL [14]
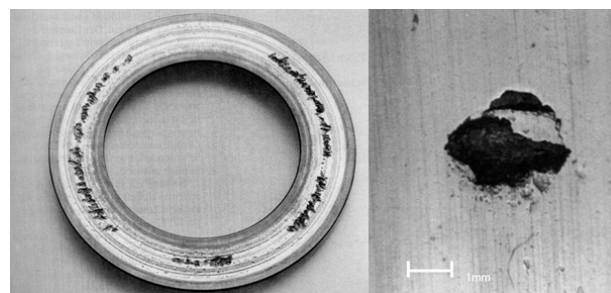
Figure 1. Pitting on a bearing ring.
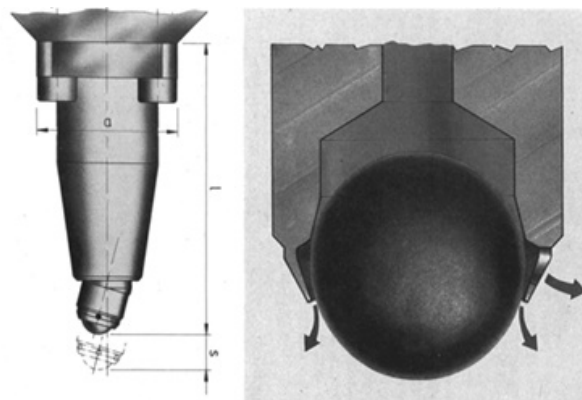
Figure 2. The HEGENSCHEIDT hydrostatic roller burnishing tool [11].

can be given as examples, in both cases, constant pressure of the roller burnishing element on the surface of the workpiece is ensured, along with a supply of process fluid to the point of contact. Convenient conditions were provided by speed values in the range of 20–100 m min^{-1}, feeds of 0.05 to 0.2 mm, and a working force derived from the fluid pressure of 500-2500 N [1, 6].

Simulation by means of the finite element method can provide a better understanding of the mechanism

TIME=2
SINT (AVG)
PowerGraphics
EFACET=1
AVRES=Mat
DMX =.004169
SMN =.781821
SMX =2801
PATH
| | 0 :21
| | 317.669
| | 635.357
| | 953.044
| | 1271
| | 1588
| | 1906
| | 2224
| | 2542
| | 2859
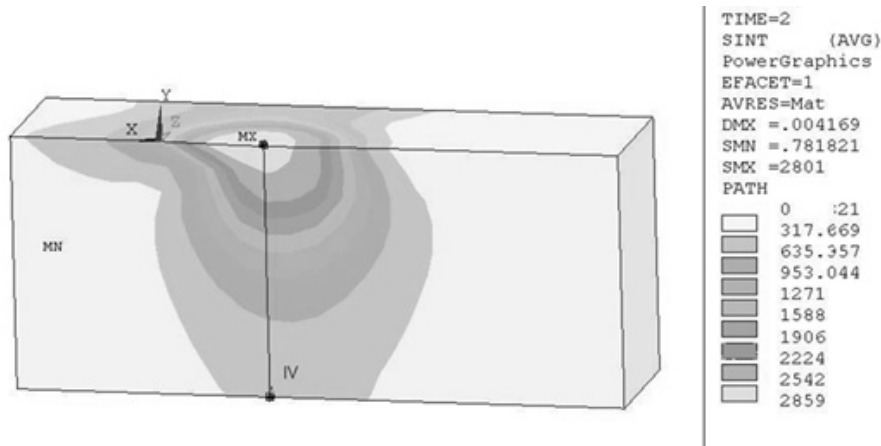
FIGURE 3. 3D simulation of roller burnishing, reduced stress affected by friction in the surface layer [MPa].

TIME=2
EPPLINT (AVG)
DMX =.004169
SMX =.013584
PATH
| | 0
| | .001509
| | .003019
| | .004528
| | .006037
| | .007547
| | .009056
| | .010565
| | .012075
| | .013584
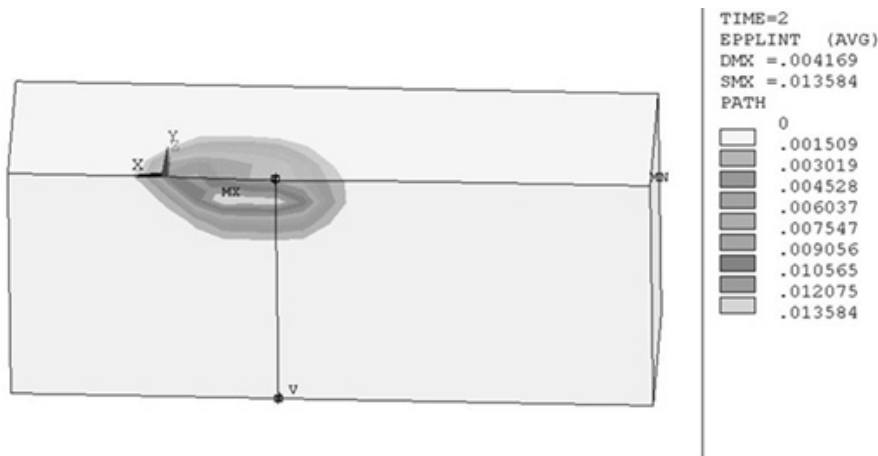
FIGURE 4. 3D simulation of roller burnishing, intensity of the plastic deformation affected by friction in the surface layer [–].

of plastic deformation in the surface layer of a roller-burnished material [3, 4]. The ANSYS program was selected as a suitable candidate, and a simulation was made of the stress and plastic deformations in the immediate vicinity of the contact point between the workpiece and the tool [12, 13].

The model itself was reduced to a depth of 0.5 mm for the workpiece, and the ball segment was reduced to a length of 0.3 mm [4].

The resultant values showed a high stress value in the vicinity of the contact point between the workpiece and the roller-burnishing element, and also showed the formation of a plastically deformed area in the surface layer, see Figs. 3 and 4. These figures present the results for a 3mm ball made from sintered carbide, and a working force of 2000 N.

The lines marked as IV and V represent the paths selected for evaluating the residual stress and the intensity of the plastic deformation below the surface, see Fig. 5. The areas marked as MX, MN represent places with maximum and minimum values.

The simulations show that the resultant course of the stress below the roller-burnishing element is also influenced to a relatively large extent by the roller-burnishing method that has been used; particularly when using a friction element, a more significant plastically deformed area is shifted to the surface of the workpiece.

The intensity of the stress and the plastic deformation [12] used in the simulation is defined by

$$\sigma_I = \max\{\sigma_1 - \sigma_2, \sigma_2 - \sigma_3, \sigma_3 - \sigma_1\},$$
$$\epsilon_I = \max\{\epsilon_1 - \epsilon_2, \epsilon_2 - \epsilon_3, \epsilon_3 - \epsilon_1\}.$$

To provide a better illustration of the course of the plastic deformation itself in the area below the tool, the cross-section of the courses can be shown, see Fig. 5.

The simulations that were performed showed an excess of stress in the surface layer of the workpiece up to a depth of roughly 0.2 mm. This leads to plastic deformation, and has a significant impact on the examined material layer.

3. Experimental measurements

For an evaluation of the actual changes in the surface layer, the residual stress was measured and the surface roughness of the roller-burnished surface was
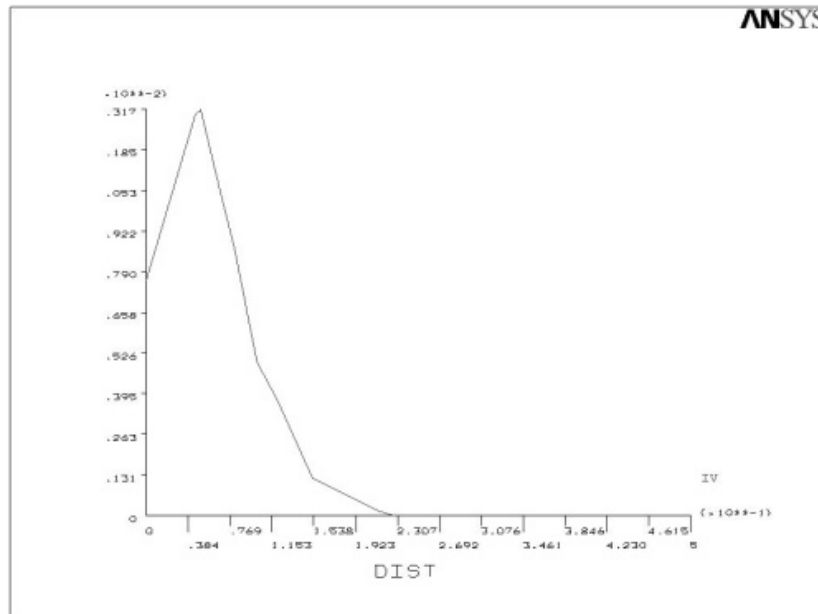
FIGURE 5. Intensity of the plastic deformation, depending on the depth below the surface.
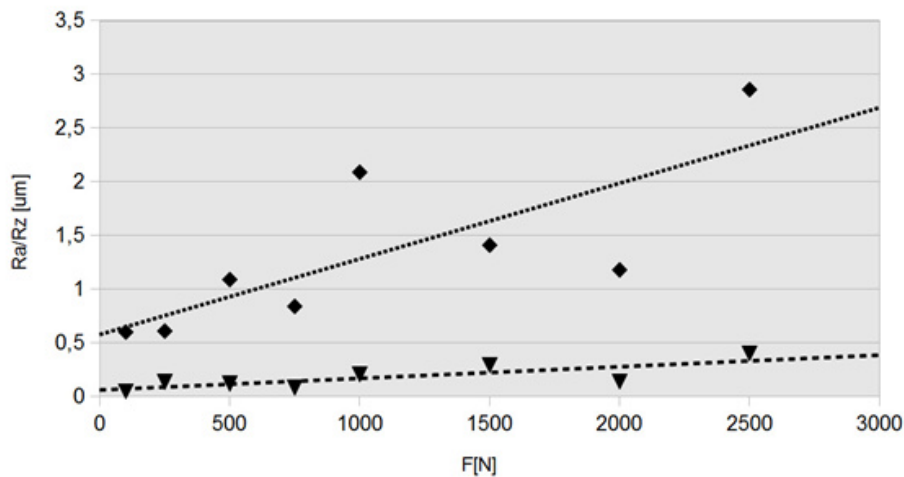
FIGURE 6. Arithmetical mean roughness R_a and maximum height of profile R_z depending on the size of working force F.

evaluated. Next, the surface layer was investigated, and images were obtained from optical and electron microscopes.

Various values of the working force acting on the forming element were tested. The forming element, made of sintered carbide, was 3 mm in diameter and spherical in shape. Various other technological parameters did not have such a major impact as the change in the working force. Working speed values of $v_k = 30 \, \mathrm{m \, s^{-1}}$ were therefore chosen, and the feed per revolution was $f = 0.05 \, \mathrm{mm}$, which corresponds to the recommended values.

The arithmetic mean roughness R_a and also the maximum height of profile R_z [6, 8] were evaluated as shown in Fig. 6.

The resulting measurements show a more signifi-

cant increase in surface roughness when the working force exceeds 1000–1500 N. However, this value still meets the parameters required for the final state of the surface of the workpiece.

The roentgenographic method also evaluates the crystal lattice deformation in the individual phases of the material under consideration [7, 10]. The Philips D500 equipment that was used also allowed an assessment of the percentage representation of each metal phase. It was therefore possible for each measurement of the residual stress to determine the amount of residual austenite in the surface layer. The resultant percentage representation value was measured with accuracy of $\pm 1\%$ of the total volume of material. However, the depth of the layer measured with this method was limited to 40 μm below the surface.
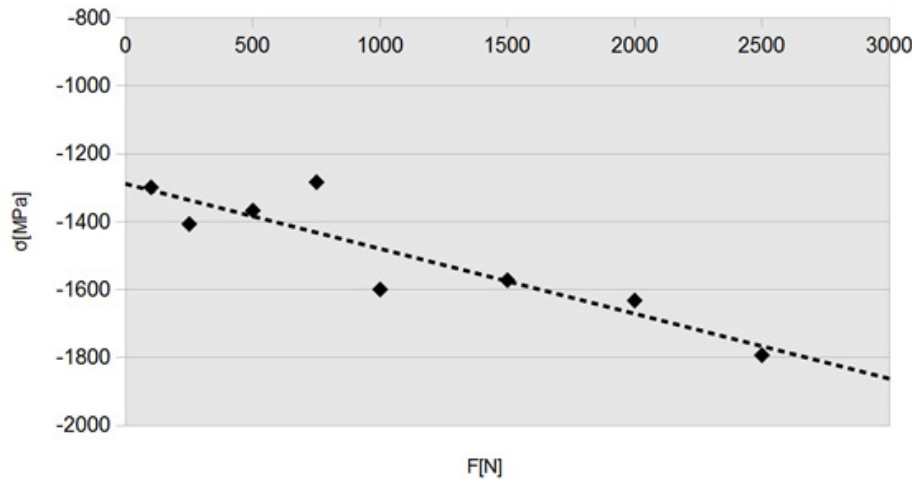
FIGURE 7. Dependence of the residual stress in the surface layer on the size of the working force.
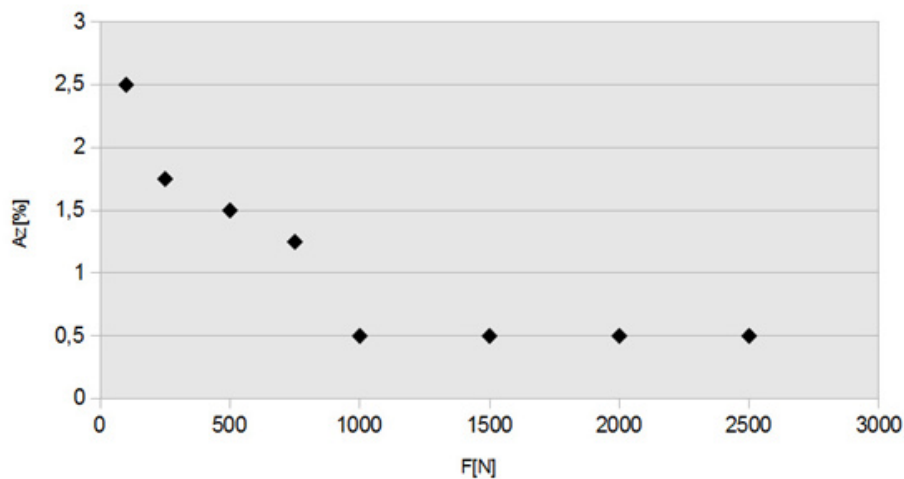
FIGURE 8. Dependence of the amount of residual austenite in the surface layer on the size of the working force.

As part of the measurements, changes to the amount of residual austenite were evaluated, depending on the size of the working force. Subsequently, the amount of residual stress was also assessed in relation to the working force [6]. Both of these dependencies are shown in Figs. 7 and 8. The negative values in Fig. 7 represent the compressive stress [7].

Within the measured interval, the pressure residual stress value rises approximately linearly with the working force.

Light and X-ray microscopy were used for evaluating the state of the structure in the surface layer. The respective steel with 1 % C, 0.4 % Mn and 1.5 % Cr is used for rolling elements and for rings up to 25 mm in thickness. Like mass-produced rings of rolling bearings, the samples were hardened and tempered at low temperature.

A comparison between the images of the subsurface layer (Fig. 9 left) and the layer a few tenths of milimetre below the surface (Fig. 9 right) shows that there is a reduction in the residual austenite areas [2, 5].

4. CONCLUSIONS

Our results lead to the conclusion that the roller-burnishing method applied here can offer significant improvements to the properties of the surface layer of dynamically-loaded bearing rings. The tested samples showed both improvements in the state of the residual stress, and also changes in the roughness of the surface layer. Significant plastic deformation occurred even though the material was in a hardened state. This result may be ascribed to a plastic deformation or a possible phase changes in the material leading to volume changes.

A positive impact on the lifetime of bearing has been experimentally verified for bearings where an additional roller-burnishing operation was applied to the rolling track. The service life of these bearings was more than doubled [11]. Due to these good results for surface roughness, it is possible to consider skipping the superfinishing operation and replacing it by roller burnishing.
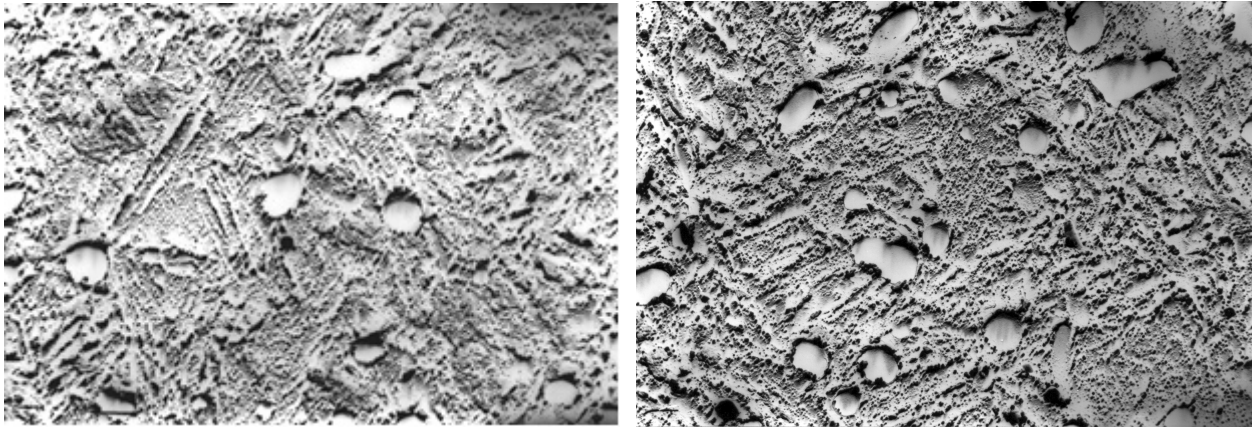
FIGURE 9. Steel for roller bearings 14109.4, 10000×, roller-burnished by a working force of 2500 N: (left) a replica at a depth of 0.2 mm below the roller-burnished surface; (right) a replica 0.01 mm below the roller-burnished surface.

REFERENCES

[1] YEN, Y.C., P. SARTKULVANICH and T. ALTAN. Finite Element Modeling of Roller Burnishing Process. *CIRP Annals - Manufacturing Technology*. 2005, vol. 54, issue 1, pp. 237-240. DOI:10.1016/s0007-8506(07)60092-4

[2] KUNDIN, Julia, Evgeny POGORELOV and Heike EMMERICH. Numerical investigation of the interaction between the martensitic transformation front and the plastic strain in austenite. *Journal of the Mechanics and Physics of Solids*. 2015, no. 76, pp. 65-83. DOI:10.1016/j.jmps.2014.12.007

[3] BALLAND, Pascale, Laurent TABOUROT, Fabien DEGRE and Vincent MOREAU. Mechanics of the burnishing process. *Precision Engineering*. 2013, vol. 37, issue 1, pp. 129-134. DOI:10.1016/j.precisioneng.2012.07.008

[4] BALLAND, Pascale, Laurent TABOUROT, Fabien DEGRE, Vincent MOREAU and Yan-wing NG. An investigation of the mechanics of roller burnishing through finite element simulation and experiments. *International Journal of Machine Tools and Manufacture*. 2013, vol. 65, pp. 29-36. DOI:10.5353/th_b3196038

[5] LEHNHOFF, G.R., K.O. FINDLEY and G.R. CHANANI. Influence of austenite stability on predicted cyclic stress-strain response of metastable austenitic steels. *Procedia Engineering*. 2011, vol. 10, pp. 1097-1102. DOI: 10.2172/4114261. Accessible from:

[6] MEZLINI, S., S. MZALI, S. SGHAIER, C. BRAHAM, Ph. KAPSA and J. MARTIN. Effect of a combined machining/burnishing tool on the roughness and mechanical properties. *Lubrication Science*. 2013, vol. 26, issue 3, pp. 175-187. DOI:10.2172/821697

[7] NEWBY, M., M. N. JAMES and D. G. HATTINGH. Finite element modelling of residual stresses in shot-peened steam turbine blades. *FFEMS*. 2014, vol. 37, issue 7, pp. 707-716. DOI:10.1111/ffe.12165

[8] DAVIM, J. Paulo. *Surface Integrity in Machining*. 1st ed. London: Springer, 2010, 215 pp. ISBN 978-1-84882-873-5.

[9] VAJSKEBR, Jiří and Zdeněk ŠPETA. *Dokončování a zpevňování povrchu strojních součástí válečkováním*. Praha: SNTL, 1984.

[10] KRAUS, Ivo and Nikolaj GANEV. *Difrakční analýza mechanických napětí*. 1st ed. Prue: ČVUT, 1995. ISBN 80-01-01366-9.

[11] ZEMČÍK, Oskar. *Změna vlastností oběžných drah valivých ložisek po aplikaci válečkování: Thesis*. Brno: CERM, 2001. 136 pp. ISBN 80-214-2131-2. Dizertační práce. VUT v Brně, FSI, ÚST.

[12] *Ansys Theory reference: v. 13* [online]. 2011. Southpointe: Ansys, Inc. [cit. 2011-07-14].

[13] LAWRENCE, Kent L. *ANSYS Workbench Tutorial: Structural & Thermal Analysis Using the ANSYS Workbench Release 12.1 Environment*. Mission: Schroff Development Corp, 2010, 252 s. ISBN 1585035807.

[14] ECOROLL AG. *ECOROLL AG Werkzeugtechnik* [online]. Celle, 2013 [cit. 2013-05-14]. http://www.ecoroll.de